

2,4-dinitrophenol downregulates genes for diabetes and fatty liver in obese mice

Qian Gao, Jiang He, Tao Liao, Qing-Ping Zeng

Whether obesity is a disease or a risk factor of chronic diseases including diabetes and fatty liver remains debating. We report here that a high-fat diet (HFD) alone or HFD and intramuscular injection of mice with a high dose (1.2 mg/kg) of lipopolysaccharide (LPS) induces the peripheral noninflammatory obesity. In contrast, HFD and intraperitoneal injection of mice with a low dose (0.25 mg/kg) of LPS induces the visceral low-grade inflammatory obesity. While the noninsulin dependent diabetes mellitus (NIDDM)- and nonalcoholic fatty liver disease (NAFLD)-related genes are globally upregulated in HFD+low-dose LPS mice, NIDDM and NAFLD genes are not extensively upregulated in HFD+high-dose LPS mice. The mitochondrial uncoupler 2,4-dinitrophenol (DNP) was found to exert a weight-reducing effect in obese mice by downregulating NF- κ B-primed inflammatory response accompanying with NIDDM and NAFLD genes, thereby abrogating inflammatory hepatic injury. In conclusion, visceral low-grade inflammatory obesity that predisposes NIDDM and NAFLD can be ameliorated by DNP via anti-inflammation.

2, 4-dinitrophenol downregulates genes for diabetes and fatty liver in obese mice

Qian Gao, Jiang He, Tao Liao, Qing-Ping Zeng

Tropical Medicine Institute, Guangzhou University of Chinese Medicine, Guangzhou, China

ABSTRACT

Whether obesity is a disease or a risk factor of chronic diseases including diabetes and fatty liver remains debating. We report here that a high-fat diet (HFD) alone or HFD and intramuscular injection of mice with a high dose (1.2 mg/kg) of lipopolysaccharide (LPS) induces the peripheral noninflammatory obesity. In contrast, HFD and intraperitoneal injection of mice with a low dose (0.25 mg/kg) of LPS induces the visceral low-grade inflammatory obesity. While the noninsulin dependent diabetes mellitus (NIDDM)- and nonalcoholic fatty liver disease (NAFLD)-related genes are globally upregulated in HFD+low-dose LPS mice, NIDDM and NAFLD genes are not extensively upregulated in HFD+high-dose LPS mice. The mitochondrial uncoupler 2,4-dinitrophenol (DNP) was found to exert a weight-reducing effect in obese mice by downregulating NF- κ B-primed inflammatory response accompanying with NIDDM and NAFLD genes, thereby abrogating inflammatory hepatic injury. In conclusion, visceral low-grade inflammatory obesity that predisposes NIDDM and NAFLD can be ameliorated by DNP via anti-inflammation.

INTRODUCTION

Although the American Medical Association (AMA) declared obesity being a disease (<http://www.ama-assn.org>), Katz (2014) argued that obesity is not a disease, but a risk factor of other chronic diseases, such as the noninsulin dependent diabetes mellitus (NIDDM) and nonalcoholic fatty liver disease (NAFLD). He insisted that not only can chronic diseases develop in the absence of obesity, but not every obese person develops any such conditions. Clinically, some obese people without inflammation are sensitive to insulin and do not develop diabetes, but

29 others with inflammation are resistant to insulin and can develop diabetes (Hawkesworth *et al.*
30 2013). Therefore, it seems that the noninflammatory obesity or “healthy obesity” does not
31 precede the chronic diseases, whereas the inflammatory obesity or “unhealthy obesity”
32 predisposes the chronic diseases (Jais *et al.* 2014).

33 It is currently much discrepant about the origin of inflammation in obesity. For example, some
34 authors suggested that increased adipocyte O₂ consumption induces hypoxia inducible factor 1 α
35 (HIF-1 α), causing inflammation and insulin resistance (Lee *et al.* 2014), but others supposed that
36 hepatic and macrophage heme oxygenase-1 (HO-1) drives the metaflammation and insulin
37 resistance (Jais *et al.* 2014). The inflammation in obesity might be attributed to either an
38 infectious origin or a noninfectious origin although some authors underscored a dual origin, in
39 which the bacterial endotoxin lipopolysaccharide (LPS) and free fatty acids (FFAs) were thought
40 to equally activate NF- κ B, thereby upregulating the proinflammatory cytokines that induce the
41 insulin resistance (Heinrichsdorff & Olefsky 2012).

42 LPS binding to Toll-like receptor 4 (TLR4) via the co-receptor CD14 has been previously
43 confirmed, but a detailed mechanism by which FFAs binding to TLR4 has been poorly
44 understood for a long time. Upon the recent finding that the liver secretory protein Fetuin A (Fet
45 A) serves as an adaptor for FFAs binding to TLR4 (Pal *et al.* 2012), it is now believed that FFAs
46 deem to elicit the inflammatory response in the high-fat diet (HFD)-induced obesity. It has been
47 concluded that saturated FFAs exert the dominant proinflammatory effects, whereas ω -3
48 polyunsaturated FFAs (PUFAs) exhibit the potent anti-inflammatory roles (Glass & Olefsky
49 2012).

50 A putative association of gut microbiota with obesity has currently evoked much enthusiasm
51 in recent years. Ding *et al.* (2010) indicated that intestinal inflammation precedes and correlates
52 with HFD-induced obesity, adiposity and insulin resistance, but the absence of gut microbiota in
53 germ-free mice blunts the upregulation of primary inflammatory indicators. Kim *et al.* (2012)
54 also revealed a relevance of HFD with gut dysbiosis by showing the overgrowth of
55 *Enterobacteriaceae*, which exacerbates inflammation and obesity in mice. A recent work further
56 indicated that adipocyte inflammation is essential for healthy adipose tissue expansion and
57 remodeling, in which visceral fat is depoted for filtering the gut-derived LPS leakage (Asterholm
58 *et al.* 2014), seemingly addressing a link between gut bacterial dysbiosis and visceral adipose
59 storage.

60 Mounting evidence has emerged that Gram negative *Bacteroides*-enhanced mucus degradation
61 is responsible for reduced gut lining integrity, thereby leading to leakage of LPS from the
62 gastrointestinal tract into the blood stream (Qin *et al.* 2012; Le Chatelier *et al.* 2013). Given that

63 LPS is an initiator of inflammatory responses, it is anticipated that the exogenous LPS injected
64 into the skeletal muscle should mimic the endogenous LPS leaked from the gut to upregulate the
65 proinflammatory cytokines. In our preliminary tests, however, we found with surprise that either
66 HFD alone or HFD combined with intramuscularly injected 1.2 mg/kg LPS can even
67 downregulate the majority of cytokines/chemokines, including the proinflammatory cytokines,
68 TNF α , IL-1 β , and INF γ . Otherwise, [Imajo *et al.* \(2012\)](#) demonstrated that a single intraperitoneal
69 injection of mice with 0.25 mg/kg LPS increases the infiltration of inflammatory cells into the
70 hepatic tissue of HFD-fed mice.

71 We thought that intraperitoneal injection with low-dose LPS could simulate the trace-amount
72 LPS leakage capable of inducing the chronic inflammation, eventually leading to the
73 inflammatory obesity. In contrast, intramuscular injection with high-dose LPS should resemble
74 the large-scale bacterial infection to initiate the acute inflammation, thereby developing the
75 noninflammatory obesity. In human, approximately 40–50% of obese adults do not develop fatty
76 liver, and the level of inflammatory biomarkers is higher in obese subjects with fatty liver
77 compared to BMI-matched subjects without fatty liver ([Zhao *et al.* 2015](#)).

78 So we compared the expression profiles of inflammatory response genes, noninsulin
79 dependent diabetes mellitus (NIDDM)-involved genes, and nonalcoholic fatty liver disease
80 (NAFLD)-related genes in HFD+high-dose LPS mice with those in HFD+low-dose LPS. As
81 results, we found that HFD+high-dose LPS induces the peripheral noninflammatory obesity with
82 hepatic high-grade inflammation, whereas HFD+low-dose HFD+LPS induces the hepatic low-
83 grade inflammatory obesity with adipose high-grade inflammation. Low-grade inflammation has
84 been defined as a two- to threefold increase in the systemic concentrations of proinflammatory
85 cytokines, such as tumor necrosis factor α (TNF α), interleukin 6 (IL6), and C-reactive protein
86 (CRP) ([Petersen & Pedersen 2005](#)).

87 Based on the obese mouse model with the visceral low-grade inflammation established by
88 HFD+0.25 mg/kg LPS, we examined whether the classic weight-reducing drug 2,4-dinitrophenol
89 (DNP) would exert a weight-reducing effect through an alternative mechanism in addition to
90 mitochondrial uncoupling, from which DNP-mediated anti-inflammation was elucidated for the
91 first time. Our data available in the present study have not only verified the presence of dose-
92 dependent LPS-driven inflammatory and noninflammatory obesity, but also disclosed the anti-
93 inflammatory response as a mechanism underlying DNP for weight loss.

94 MATERIAL AND METHODS

95 **Animals and experimental procedures**

96 Kunming (KM) mice, belonging to an outbred population originated from SWISS mice, were
97 used. All mice were housed on a 12-h light: 12-h dark cycle at 25°C, and fed with either HFD
98 (60% basic feed-stuff + 20% lard + 10% sucrose + 10% yolk) or *ad libitum* chow (AL).
99 HFD+1.2 mg/kg LPS mice were first fed with AL for two weeks, and then fed with HFD for two
100 months, during which 1.2 mg/kg LPS was injected into the hind-leg muscle (Islam & Pestka
101 2006) one day before sampling. HFD+0.25 mg/kg LPS mice were first fed with AL for two
102 weeks, and then fed with HFD for 1.5 months, during which 0.25 mg/kg LPS was injected into
103 peritoneal (Imajo *et al.* 2012) from the 5th week of HFD feeding with the regimen of injection on
104 every two days for two weeks. For drug treatment, mice were intraperitoneally injected daily
105 with 16 mg/kg DNP for two weeks. Animal procedures were in accordance with the animal care
106 committee at the Guangzhou University of Chinese Medicine, Guangzhou, China. The protocol
107 was approved by the Animal Care Welfare Committee of Guangzhou University of Chinese
108 Medicine (Permit Number: SPF-2011007).

109 **Quantitative polymerase chain reaction (qPCR)**

110 Total RNA was extracted by a Trizol method. The target gene *NF-κB* was amplified with a
111 forward primer, CGACAACATCTCCTTGGCTGGCT, and a reverse primer,
112 GGGTCTGCTCCTGCTGCTTTG. The house-keeping gene *GAPDH* was amplified with a
113 forward primer, GGAGAAACCTGCCAAGTATGATGAC, and a reverse primer,
114 GAGACAACCTGGTCCTCAGTGTA. The copy numbers of amplified genes were estimated by
115 $2^{-\Delta\Delta Ct}$, in which $\Delta\Delta Ct = [\text{target gene (treatment group)} / \text{target gene (control group)}] /$
116 $[\text{housekeeping gene (treatment group)} / \text{housekeeping gene (control group)}]$.

117 **RT-PCR array**

118 The RT² Profiler™ PCR Array Mouse Fatty Liver (PAMM-157Z) was purchased from
119 SABioscience Qiagen, Hilden, Germany, and Quantibody® Mouse Cytokine Antibody Array
120 4000 was purchased from RayBiotech, Inc, Norcross, GA, USA. The experiments were
121 performed respectively by Kangchen Biotechnology Co, Ltd, Shanghai, China, and RayBiotech,
122 Inc. Guangzhou, China.

123 **Cytokine antibody array**

124 Protein extraction from blood cells by Cell & Tissue Protein Extraction Reagent (KangChen KC-
125 415) was conducted according to the manufacturer's instruction. Cytokine antibody array was
126 carried out by Kangchen Bio-Tech, Shanghai, China using RayBio® Mouse Cytokine Antibody

127 Array.

128 **Enzyme-linked immunosorbent assay (ELISA)**

129 The target proteins including insulin, leptin, and NF- κ B as compared to the reference protein
130 GAPDH were immunoquantified by ELISA kits manufactured by Shanghai Yuanye Bio-
131 Technology Co., Ltd, Shanghai, China according to manufacture's manuals.

132 **Serological tests**

133 Triglycerides, total cholesterol, aspartate transaminase (AST), and alanine tranaminase (ALT)
134 were determined by ECHO Automatic Chemistry Analyzer, I.S.E. S.r.l., Via delle Driadi, Roma,
135 Italy. The reagent kits were purchased from Shanghai Kehua Laboratory System Co, Ltd,
136 Shanghai, China.

137 **Histopathological analysis**

138 A piece of the tissue was fixed by 10% formaldehyde followed by paraffin embedding and
139 haematoxylin-eosin (HE) staining. The degenerative scores of inflammatory lesions were
140 recorded as: 1-2 points - mild/severe hydropic degeneration; 3-4 points - mild/severe adipose
141 degeneration; 5 points - necrosis.

142 **Selective bacterial culture**

143 The selective cultural media of EMB agar powders for *Escherichia coli*, LBS agar powders for
144 *Lactobacillus*, and TPY agar powders for *Bifidobacterium* were purchased from Qingdao Hope
145 Bio-Technology Co. Qingdao, China. Selective bacterial culture was performed in the anaerobic
146 jar and AnaeroGen paper sachets from OXOID, UK, according to the manufacture's instructions.

147 **Determiration of lactic acid, NO and 3NT levels**

148 Lactic acid (LA) and NO levels were determined using the reagent kits manufactured by
149 Jiancheng Biotechnology Institute, Nanjing, China. The LA level (mM) = (OD test – OD
150 blank)/(OD standard – OD blank) • standard LA concentration (3 mM) • sample dilution folds.
151 The NO level (μ M) = (OD test – OD blank)/(OD standard – OD blank) • standard nitrate
152 concentration (20 μ M). The 3NT content was measured by the reagent kit manufactured by
153 Shanghai Westang Bio-Tech Co, Ltd, Shanghai, China. The 3NT content (μ g/mg) = 3NT
154 concentration (μ g/mL)/protein concentration (mg/mL), in which 3NT concentration was
155 calculated from the regression formula: $y=(0.372x - 0.016, R^2=1.000)$.

156 **Statistical analysis**

157 Statistical analyses were conducted by the one-way ANOVA method using SPSS version 17.0
158 for Windows. All data were represented as mean \pm SEM unless otherwise stated. The XY graphs
159 and column graphs were plotted and depicted using GraphPad Prism version 4.0.

160 RESULTS

161 Peripheral noninflammation in HFD-fed obese mice with intramuscular injection of 1.2 162 mg/kg LPS

163 To decipher the etiological cause of inflammation in obesity, we assumed that HFD alone is
164 sufficient to induce gut dysbiosis, LPS leakage, and inflammatory obesity, during which
165 challenges with the exogenous LPS should accelerate such a process. So we firstly intended to
166 reveal whether HFD would lead to gut dysbiosis by enhancing the overgrowth of specific
167 bacteria. By collecting the fecal samples of HFD-fed mice and selectively culturing the
168 commensal gut microbiota, including *E. coli*, *Lactobacillus*, and *Bifidobacterium*, we confirmed
169 that the colony numbers of *E. coli* overwhelm those of *Lactobacillus* and *Bifidobacterium*, but
170 there is no significant difference in colony numbers of *Lactobacillus* from those of
171 *Bifidobacterium* (Figure 1A). Furthermore, we also noticed that intramuscular injection of mice
172 with LPS or LPS-containing complete Freund's adjuvant (CFA) can potently induce the serum
173 high-level NO, whereas live yeast feeding does not elevate the serum NO level (Figure 1B),
174 implying that *E. coli*-produced LPS can initiate the inflammatory response and trigger NO burst.

175 To ensure how many times of LPS challenges are suitable to potentiate the inflammatory
176 responses, we simply monitored the serum NO production and the muscular 3NT formation after
177 multiple intramuscular injections of mice with 1.2 mg/kg LPS. Consequently, a gradual
178 reduction of the NO level was observed after injection of mice with 1.2 mg/kg LPS in the 14-day
179 durations and four-time injections (Figure 1C), suggesting a gradual compromise of the
180 inflammatory response to LPS. Similarly, we also noticed a significant decrease of the 3NT
181 content after the prime-boost LPS inoculation (Figure 1D). So a singular injection other than
182 multiple injections should be preferred to prompt the progression to LPS-driven inflammatory
183 obesity.

184 As illustrated in Figure 1E, both HFD mice and HFD+1.2 mg/kg LPS mice become obese with
185 the heavier body weight and higher body adipose percentage after fed with HFD for 1.5-2
186 months (Figure 1E and 1F). Logically, we anticipated that the proinflammatory cytokines should
187 be upregulated in both HFD-fed obese mice and LPS-injected HFD obese mice. Surprisingly, we
188 found that the expression levels of all examined 40 cytokines and chemokines in the skeletal

189 muscle of either HFD mice or HFD+1.2 mg/kg LPS mice are totally unchanged or even lower
190 than those in AL mice (Figure 1G, see also Table S1). Among the most common
191 proinflammatory cytokines, IL-1 β in HFD mice maintains an equivalent level with AL mice
192 (0.95-fold changes), whereas it is much lower in HFD+1.2 mg/kg LPS mice than in AL mice
193 (0.16-fold downregulation). While TNF α is almost unchanged in HFD mice or slightly
194 downregulated in HFD+1.2 mg/kg LPS mice (0.95- and 0.85-fold changes), IFN γ is dramatically
195 downregulated in both obese mice (0.11- and 0.05-fold downregulation).

196 The possible reasons on the downregulation of proinflammatory cytokines in HFD mice or
197 HFD+1.2 mg/kg LPS mice might be attributed to antibody neutralization or immune suppression.
198 In fact, it was previously found that a single optimal immunogenic dose of LPS can trigger an
199 antibody response (Hiernaux *et al.* 1982), and anti-LPS antibodies can reduce the plasma LPS
200 titers in humans (Wells *et al.* 1990). Recently, a high dose of LPS was validated to be an
201 immunosuppressor (Kelly *et al.* 2012). Therefore, either HFD alone or HFD+1.2 mg/kg LPS can
202 only induce the peripheral/subcutaneous noninflammatory obesity in mice.

203

204 **Visceral high-grade inflammation in HFD-fed obese mice with intramuscular injection of** 205 **1.2 mg/kg LPS**

206 To investigate whether HFD+1.2 mg/kg LPS would cause the visceral inflammation, we
207 quantified the hepatic inflammatory response transcripts and NIDDM-involved transcripts
208 among 84 NAFLD-related transcripts in HFD mice and HFD+1.2 mg/kg LPS mice (Table 1, see
209 also Table S2).

210 From the data listed in Table 1, it can be clearly noticed that HFD+1.2 mg/kg LPS can
211 stimulate a potent hepatic inflammatory response, in which the most common proinflammatory
212 cytokine transcripts, including *Il1b* mRNA (94.24 folds), *Il6* mRNA (12.54 folds), and *Tnf*
213 mRNA (10.24 folds), are extremely upregulated compared with AL mice. However, HFD
214 differentially allows the proinflammatory cytokines to be unchanged (*Tnf* mRNA for 1.15 folds),
215 mildly upregulated (*Il1b* mRNA for 6.46 folds), or slightly downregulated (*Ifng* mRNA for -5.21
216 folds). In HFD+1.2 mg/kg LPS mice, the anti-inflammatory cytokine transcript *Il10* mRNA is
217 dramatically upregulated for 50.20 folds, and the dual anti-/proinflammatory cytokine *Il6* mRNA
218 is also considerably upregulated for 12.54 folds. On the other hand, *Il10* mRNA exhibits 4.32-
219 fold upregulation and *Il6* mRNA shows unchanged expression (1.51 folds) in HFD mice.

220 In regard to the NIDDM transcripts, HFD+1.2 mg/kg LPS mice have two kinds of mRNAs

221 (*Socs3* and *Xbp1* mRNAs) being higher than AL mice for over two folds, whereas HFD mice
222 have only one kind of mRNA (*Xbp1* mRNA) being higher than AL mice for over two folds. It
223 has been demonstrated that SOCS3 (suppressor of cytokine signaling-3) is responsible for the
224 specific inhibition of Janus kinases (JAKs), suggesting an implication in the suppression of
225 cytokine signaling (Babon *et al.* 2012). XBP1 (X-box binding protein 1) was also proved to be
226 implicated in the compromise of stress from endoplasmic reticulum (ER) and mitigation of
227 susceptibility to inflammatory processes (Casus-Tinto *et al.* 2011).

228 It can be briefly summarized that HFD+1.2 mg/kg LPS induce the hepatic high-grade
229 inflammation because their expression levels of proinflammatory cytokines are highly elevated
230 for more than 2-3 folds. Meanwhile, HFD+1.2 mg/kg LPS also upregulates some NIDDM genes
231 beneficial for anti-inflammation. Taken together, these results demonstrated that HFD+1.2
232 mg/kg LPS can induce obesity with the peripheral noninflammation but visceral high-grade
233 inflammation, which might resemble the acute pathogenic infection and would eventually lead to
234 the immune deprival of LPS in the blood circulation.

235

236 **Visceral low-grade inflammation in HFD-fed obese mice with intraperitoneal injection of** 237 **0.25 mg/kg LPS**

238 To avoid the immune depletion of LPS, we replaced the high-dose and short-term LPS exposure
239 by the low-dose and long-term LPS exposure, i.e., the injection dose was changed from 1.2
240 mg/kg LPS to 0.25 mg/kg LPS, the injection procedure was changed from the intramuscular
241 injection to the intraperitoneal injection, and the injection frequency was changed from only one
242 injection to multiple injections. Other authors have reported that the infiltration of inflammatory
243 cells are enhanced in the liver tissue of HFD-fed mice after treatment by 0.25 mg/kg LPS (Imajo
244 *et al.* 2012).

245 After multiple LPS injections on every two days for two months from the 5th week of HFD
246 feeding, HFD+0.25 mg/kg LPS mice become obese than AL mice (Figure 2A). The LA level that
247 indicates a hypoxic state is as expected higher in HFD+0.25 mg/kg LPS mice than that in AL
248 mice (Figure 2B). Accordingly, HFD+0.25 mg/kg LPS mice show the extremely increased
249 adipose expression levels of as many as 200 cytokines/chemokines, among which those with the
250 upregulated levels above 100 folds compared with AL mice were illustrated (Figure 2C). For
251 example, IL-1 β mRNA is elevated for 3477 folds, and TNF α mRNA is increased for 546 folds.
252 While AL mice does not exhibit the acute hepatic injury (Figure 2D), hepatic inflammatory
253 pathogenesis could be seen in HFD+0.25 mg/kg LPS mice albeit with only one-point

254 inflammatory score (Figure 2E).

255 Intriguingly, the hepatic inflammatory response transcripts in those obese mice exhibit the
256 restricted upregulation for only 2- to 3-folds, which are well coincided with the definition of low-
257 grade inflammation (Petersen & Pedersen 2005). Importantly, there are also as many as six
258 NIDDM transcripts showing the similarly restricted upregulation for 2-4 folds in the hepatic
259 tissue of HFD+0.25 mg/kg LPS mice (Table 2, see also Table S3).

260 From above results, we can draw a conclusion that HFD+0.25 mg/kg LPS can extensively
261 induce the inflammatory response genes and NIDDM genes, in which the fold changes of
262 proinflammatory cytokines are extremely upregulated in the adipose tissue, but restrictively
263 upregulated in the hepatic tissue. So it was understandable that HFD+0.25 mg/kg LPS through
264 multiple intraperitoneal injections can dually induce the hepatic low-grade inflammation and
265 adipose high-grade inflammation in obese mice. From the minimal hepatic injury, it seems that
266 the adipose high-grade inflammation might have been abrogated as soon as possible, like the
267 acute pathogenic infection.

268

269 **DNP reduces adipose deposits without elevated transaminase activity and detectable acute** 270 **hepatic injury**

271 By the multiple intraperitoneal injections of HFD+0.25 mg/kg mice with 16 mg/kg DNP for two
272 weeks, we observed that the body adipose percentage is dramatically decreased to a lower level
273 similar with AL mice (Figure 3A). However, DNP was not found to affect the body liver
274 percentage of HFD+0.25 mg/kg mice (Figure 3B). The concentrations of triglycerides and total
275 cholesterols were not noticed to be changed by DNP although an elevated level of the total
276 cholesterol was seen in HFD+0.25 mg/kg mice (Figure 3C and 3D). Noticeably, DNP does not
277 significantly alter the serum levels of AST and ALT (Figure 3E and 3F). Compared with AL
278 mice without hepatic injury (Figure 3G) and HFD+0.25 mg/kg mice with 3-point scores
279 indicating focal necrosis (Figure 3H), DNP-treated HFD+0.25 mg/kg mice does not cause any
280 detectable hepatic inflammatory lesions (Figure 3I), suggesting that DNP might possess an anti-
281 inflammatory effect but not exert any hepatic cytotoxicity.

282

283 **DNP downregulates insulin but upregulates leptin, accompanying with downregulated NF-** 284 **κB and CD14**

285 Accompanying with adipose reduction, it was observed that insulin (INS) and leptin (LEP) are
286 synchronously modulated by DNP, in which the concentration of INS equal to that in AL mice
287 was noticed in the weight-reducing mice after injection with DNP (Figure 4A). On the other
288 hand, the concentration of LEP higher than that in AL mice was observed in the weight-reducing
289 mice upon treated by DNP (Figure 4B). Those results indicated the blood sugar sensing is
290 increased and the satiety to normal is recovered in the weight-reducing mice.

291 NF- κ B, a transcript factor initiating global inflammatory responses in all types of cells, is
292 known to be activated by numerous external signals through the interaction of a specific ligand
293 with a corresponding receptor. For example, TLR4 is such a receptor for binding LPS or FFA,
294 during which the co-receptor CD14 or the adapter FetA is necessary for initiating NF- κ B-
295 activated proinflammatory responses (Heinrichsdorff & Olefsky 2012). In our experiments, a
296 tremendous elevation and a extremely decline of *NF- κ B* mRNA were notably observed in
297 untreated and DNP-treated obese mice, respectively (Figure 4C). In parallel, a high level and a
298 lower level of NF- κ B were also measured in untreated and DNP-treated obese mice, respectively
299 (Figure 4D). Those results suggest that NF- κ B might be highly inducible.

300 To investigate whether CD14 and FetA are modulated by LPS and FFA or affected by DNP, we
301 quantified the levels of CD14 and FetA in obese mice prior to and post treatment by DNP. As
302 results, CD14 is downregulated in untreated obese mice, but upregulated in DNP-treated obese
303 mice (Figure 4E), suggesting high-level LPS in untreated mice and low-level LPS in treated
304 obese mice. On the other hand, we found that FetA is nearly unchanged in both untreated and
305 treated obese mice (Figure 4F), indicating a minor regulatory role on the induction of NF- κ B
306 exerted by FFA in the present study.

307

308 **DNP downregulates adipose proinflammatory cytokine genes and hepatic NAFLD and** 309 **NIDDM genes**

310 As compared with the adipose tissue of untreated obese mice, DNP maximally decreases the
311 proinflammatory cytokine transcripts in the adipose tissue of treated obese mice. Notably, IL-1 β
312 mRNA and TNF α mRNA were unable to detectable after treatment by DNP, in which IL-1 β
313 mRNA is declined for more than 3000 folds, and TNF α mRNA is declined for more than 500
314 folds. Among 200 examined adipose cytokines/chemokines mRNAs, DNP downregulates almost
315 all of them, in which the declined levels over 500 folds were depicted in Figure 5A. It is
316 currently obscure why DNP can exert an anti-inflammatory role although a recent report has
317 indicated that no effect of DNP was found on the plasma markers of inflammation (Perry *et al.*

318 2015). However, it seems understandable that DNP might downregulate the proinflammatory
319 cytokines by downregulating TNF α because NF- κ B can be activated by TNF α via TNFR1
320 (Baker *et al.* 2011).

321 Interestingly, DNP also downregulates a majority of NAFLD genes in the hepatic tissue of
322 obese mice, in which those transcripts with twofold changes were illustrated in Figure 5B. It was
323 predominantly that *Lepr* mRNA encoding leptin receptor and *Igfbp1* mRNA encoding insulin-
324 like growth factor binding protein 1 are downregulated for 17.93 and 10.83 fold, respectively,
325 implying an increased sensitivity to leptin and IGF. As to *CD36* mRNA encoding a fatty acid
326 translocase that determines the taste of fatty acids, its upregulation (17.01 folds) might represent
327 an increase of taste sensitivity. CD36 was found to be downregulated in the taste bud cells of
328 obese sand rats compared to lean controls (Abdoul-Azize *et al.* 2013).

329 To clearly exhibit the improvement of NIDDM gene expression profile in obese mice treated
330 by DNP, the up/downregulation of NIDDM transcripts in the hepatic tissue of DNP-treated obese
331 mice, untreated obese mice, and AL mice were listed as Table 3 (see also Table S4).

332 From the fold changes of expression levels, it was unambiguously indicated that the most of
333 NIDDM transcripts are downregulated to reach or below the levels seen in AL mice. For
334 example, *Gck* mRNA is less abundant in DNP-treated obese mice than untreated obese mice for
335 4.29 folds, and DNP-treated obese mice have a similar *Gck* mRNA level (1.02 folds) with AL
336 mice. Additionally, *Slc2a4* (*Glut4*) mRNA encoding glucose transporter 4 and *Tnf* mRNA
337 implicated in the inflammatory response are also declined in comparison of DNP-treated mice
338 with untreated obese mice and AL mice, implying a declined blood sugar level and attenuated
339 inflammatory response.

340 Besides, *Pik3r1* mRNA that codes for phosphatidylinositol 3-kinase is upregulated in DNP-
341 treated obese mice. Phosphatidylinositol 3-kinase has been noted to play a role in the metabolic
342 action of insulin, and a mutation in this gene is associated with insulin resistance (Kapeller *et al.*
343 1995). So DNP-mediated upregulation of *Pik3r1* mRNA would benefit to overcome insulin
344 resistance.

345 DISCUSSION

346 A logical relevance of HFD to inflammation is likely that HFD allows the overgrowth of
347 *Bacteroides* that enable the secretion of mucin-degrading sulfatase, which reduces gut integrity,
348 enhance LPS leakage, and elicit inflammatory responses (Qin *et al.* 2012; Le Chatelier *et al.*
349 2013). In the present study, however, we found that proinflammatory cytokines examined are

350 unchanged in the skeletal muscle of HFD-fed obese mice although LPS-releasing *E.coli* is
351 overloaded in the gut of HFD mice. The explanation to this peripheral noninflammatory obesity
352 seems that the gut lining of obese mice typically remains intact and LPS is hardly leaked into the
353 blood stream. To mimic LPS leakage, therefore, we injected the skeletal muscle of HFD mice
354 with 1.2 mg/kg LPS. Surprisingly, we did not note any downregulation of the proinflammatory
355 cytokines tested in the skeletal muscular tissue of HFD+1.2 mg/kg LPS mice. It might be able to
356 decipher such a phenomenon by antibody neutralization (Hiernaux *et al.* 1982; Wells *et al.* 1990)
357 and/or immune suppression (Kelly *et al.* 2012) because consecutive challenges with 1.2 mg/kg
358 LPS can gradually mitigate NO burst and 3NT formation triggered by inflammatory responses.
359 Therefore, HFD or HFD+1.2 mg/kg LPS only induces the obesity without peripheral
360 inflammation in mice.

361 Nevertheless, almost all quantified transcripts of the proinflammatory cytokines exhibit the
362 extreme elevation higher than five folds in the hepatic tissue of HFD+1.2 mg/kg LPS mice,
363 suggesting a simulation of the acute inflammation, which can be considered the high-grade
364 inflammation (Petersen & Pedersen 2005). As described earlier, we observed that live *E. coli*
365 feeding can dramatically downregulate the proinflammatory cytokines and sharply decline the
366 NO and LA levels (Bao *et al.* 2012). From the present study, we observed the gradual declines of
367 NO and 3NT levels in the peripheral tissue during the prime-boost challenges with 1.2 mg/kg
368 LPS, so we believed that the acute inflammatory presentation should be eventually attenuated in
369 the LPS-challenged subjects. This anticipation should be real because no extensive upregulation
370 of NIDDM and NALFD genes were detected, and no severe hepatic inflammatory injury was
371 observed in HFD+1.2 mg/kg LPS mice.

372 Although the high-grade inflammation in the adipose tissue of HFD+0.25 mg/kg LPS mice
373 should not be maintained like the acute inflammation, the low-grade inflammation must remain
374 to result in a mild but sustained hepatic inflammatory lesion. It was noticeably from the large-
375 scale upregulation of NIDDM and NALFD genes. In particularly, the inflammatory response
376 genes are upregulated for only 2-3 folds, which can be classified as the low-grade inflammation
377 (Petersen & Pedersen 2005). So HFD+0.25 mg/kg LPS can induce visceral low-grade
378 inflammation obesity in mice.

379 We did not observed the upregulation of Fet A responsible for binding of FFAs to TRL4 in
380 HFD+0.25 mg/kg LPS mice, implying irrelevance of HFD-derived FFAs to Fet A. Interestingly,
381 a recent report has delineated that the disruption of Fat A expression renders animals more
382 susceptible to endotoxemia, whereas supplementation with Fet A confers protection against
383 lethal endotoxemia (Li *et al.* 2011), suggesting an elevation of Fet A due to LPS accumulation.

384 Alternatively, saturated FFAs have been confirmed to stimulate adenine nucleotide translocase 2
385 (ANT2), an inner mitochondrial membrane protein, which leads to an uncoupled respiratory state
386 (Lee *et al.* 2014). Additionally, palmitic acid has been validated to be responsible for the
387 downregulation of vascular endothelial growth factor (VEGF) in obesity (Shimizu *et al.* 2014).
388 Therefore, it remains uncertain whether HFD triggers inflammation via FFAs in addition to LPS.

389 It has been previously demonstrated that the chronic blockade of iNOS by the *L*-arginine
390 analogue inhibitor *L*-NG-monomethylarginine (*L*-NMMA) reduces adiposity and improves
391 insulin resistance in HFD-induced obese mice (Tsuchiya *et al.* 2007). When iNOS is upregulated
392 by inflammation, eNOS should be downregulated due to an unfavorable competition with a
393 limited supply of the substrate *L*-arginine, and a deficiency of eNOS-derived NO should in turn
394 block mitochondrial biogenesis (Wang *et al.* 2015), thereby resulting in enhanced adipose
395 whitening and reduced energy expenditure, eventually leading to overweight/obesity. This is
396 because the brown adipose tissue (BAT) are converted to the white adipose tissue (WAT), which
397 usually emerges in the adipose tissue due to the progressive decrease of mitochondria (Shimizu
398 *et al.* 2014).

399 The classic anti-inflammatory agent salicylate, a degraded product of aspirin, has been
400 reported to reduce the circulating lipids in obese rats and improves the insulin sensitivity (Yuan
401 *et al.* 2001). Similarly, nitro-aspirin has also therapeutic potential for NAFLD (Ibrahim *et al.*
402 2011). Mechanically, aspirin has validated to ameliorate type 2 diabetes as an activator of
403 adenosine monophosphate-activated kinase (AMPK) (Hawley *et al.* 2012). It has been currently
404 shown that metformin and salicylate can synergistically activate liver AMPK to inhibit
405 lipogenesis and improve insulin sensitivity (Ford *et al.* 2015). DNP was previously known to
406 induce the expression of AMPK and phosphorylation of p38 MAPK (Pelletier & Coderre 2007),
407 so it should be reasonable that DNP can play a weight loss role.

408 Interestingly, we have recently reported that the NO donor sodium nitroprusside and the NO
409 precursor *L*-arginine can serve as the activators of AMPK, which in turn upregulates eNOS for
410 triggering mitochondrial biogenesis (Wang *et al.* 2015). We therefore suggested that DNP might
411 exert a weight-reducing effect via a dually tuned mechanism underlying upregulating AMPK for
412 mitochondrial biogenesis and downregulating NF- κ B for anti-inflammation, as illustrated in
413 Figure 6.

414 The healthy obesity can be classified as the adiposity with a high body mass index (BMI) but
415 without the low-grade inflammation and insulin resistance, whereas the unhealthy obesity is
416 categorized as the adiposity with a high BMI, accompanying with the low-grade inflammation,
417 and probably exhibiting insulin resistance or type 2 diabetes. It has been suggested that the

418 elevation of inflammation-induced HIF-1 α (Lee *et al.* 2014) or HO-1 (Jais *et al.* 2014) can be
419 considered a hallmark in human discriminating healthy obesity with insulin sensitivity from
420 unhealthy obesity with insulin resistance. The chronic inflammation is most likely derived from
421 an interaction of HFD with Gram negative bacteria, during which HFD-elicited gut dysbiosis
422 might lead to decreased gut lining integrity and increased LPS leakage and even endotoxemia.
423 Upon the upregulation of proinflammatory cytokines via activating NF- κ B, LPS can induce the
424 expression of iNOS, leading to potent NO burst, metabolic hypoxia, and adipogenesis.

425 Activation of iNOS predisposes inactivation of eNOS due to a restriction of the common
426 substrate *L*-arginine. Consequently, deficiency of eNOS-derived NO would suppress the
427 mitochondrial biogenesis and accelerate the adipose whitening, in which BAT is gradually
428 converted to WAT. DNP can exert the anti-obese effects by inactivating iNOS and decreasing
429 the high-level NO towards adipogenesis, and synchronously activating eNOS and increasing the
430 low-level NO for mitochondrial biogenesis and adipose browning, during which WAT can be
431 recovered to BAT. Additionally, eNOS-derived NO can inhibit NF- κ B (Clancy *et al.* 2004),
432 thereby downregulating proinflammatory cytokines and compromising inflammatory responses.

433 Despite DNP was earlier used as a weight-reducing drug, it was later discarded due to
434 intractable toxicity. The LD₅₀ of DNP in mice, rats, or cats is shown to be 30, 45, or 75 mg/kg,
435 but the lowest-observed-adverse-effect level (LOAEL) in human to be 2 mg/kg
436 (<http://www.epa.gov/ttnatw01/hlthef/dinitrop.html>). It has been reported that a very low
437 intracellular concentration of DNP, 75-fold lower than a toxic DNP level (a dose of 25 mg/kg or
438 a peak plasma concentration of 380 μ M), is sufficient to achieve significant weight-reducing
439 effects without any systemic toxicities (Perry *et al.* 2013).

440 To minimize the toxicity of DNP, we would further evaluate the weight-reducing effects of low
441 doses of nontoxic DNP in the future.

442 Conclusively, we have successfully established an obese mouse model with visceral low-grade
443 inflammation using HFD+0.25 mg/kg LPS, and also revealed for the first time that the well-
444 known mitochondrial uncoupler DNP can exert an anti-inflammatory effect for downregulation
445 of genes responsible for NIDDM and NAFLD during weight loss.

446

447 ACKNOWLEDGEMENTS

448 We thank Kangchen Biotechnology Co, Shanghai, China for performance of RT-PCR array

449 experiments. We also thank Ms. Da-Ting Wang and Ms. Pei Wu for their technical assistance.

450

451 REFERENCES

452 **Abdoul-Azize S, Atek-Mebarki F, Bitam A, Sadou H, Koceir EA, Khan NA. 2013.** Oro-gustatory
453 perception of dietary lipids and calcium signaling in taste bud cells are altered in nutritionally obesity-prone
454 *Psammomys obesus*. *PLoS ONE* **8**:e68532

455 **Asterholm IW, Tao C, Morley TS, Wang QA, Delgado-Lopez F, Wang ZV, Scherer PE. 2014.** Adipocyte
456 inflammation is essential for healthy adipose tissue expansion and remodeling. *Cell Metab* **20**:103-118

457 **Babon JJ, Kershaw NJ, Murphy JM, Varghese LN, Laktyushin A, Young SN, Lucet IS, Norton
458 RS, Nicola NA. 2012.** Suppression of cytokine signaling by SOCS3: characterization of the mode of
459 inhibition and the basis of its specificity. *Immunity* **36**:239-250

460 **Baker RG, Hayden MS, Ghosh S. 2011.** NF- κ B, Inflammation, and Metabolic Disease. *Cell Metab* **13**:11-22

461 **Bao F, Wu P, Xiao N, Qiu F, Zeng Q-P. 2012.** Nitric oxide-driven hypoxia initiates synovial angiogenesis,
462 hyperplasia and inflammatory lesions in mice. *PLoS ONE* **7**:e34494

463 **Casus-Tinto S, Zhang Y, Sanchez-Garcia J, Gomez-Velazquez M, Rincon-Limas DE, Fernandez-Funez
464 P. 2011.** The ER stress factor XBP1s prevents amyloid- β neurotoxicity. *Hum Mol Genet* **20**:2144–2160

465 **Clancy RM, Gomez PF, Abramson SB. 2004.** Nitric oxide sustains nuclear factor kappa B activation
466 in cytokine-stimulated chondrocytes. *Osteoarthritis Cartilage* **12**:552-558

467 **Ding S, Chi MM, Scull BP, Rigby R, Schwerbrock NM, Magness S, Jobin C, Lund PK. 2010.** High-fat
468 diet: bacteria interactions promote intestinal inflammation which precedes and correlates with obesity and
469 insulin resistance in mouse. *PLoS One* **5**:e12191

470 **Ford RJ, Fullerton MD, Pinkosky SL, Day EA, Scott JW, Oakhill JS, Bujak AL, Smith BK, Crane JD,
471 Blümer RM, et al. 2015.** Metformin and salicylate synergistically activate liver AMPK, inhibit lipogenesis
472 and improve insulin sensitivity. *Biochem J* **468**:125-132

473 **Glass CK, Olefsky JM. 2012.** Inflammation and lipid signaling in the etiology of insulin resistance. *Cell
474 Metab* **15**:635-645

475 **Hawkesworth S, Moore SE, Fulford AJ, Barclay GR, Darboe AA, Mark H, Nyan OA, Prentice AM.
476 2013.** Evidence for metabolic endotoxemia in obese and diabetic Gambian women. *Nutr Diabetes* **3**:e83

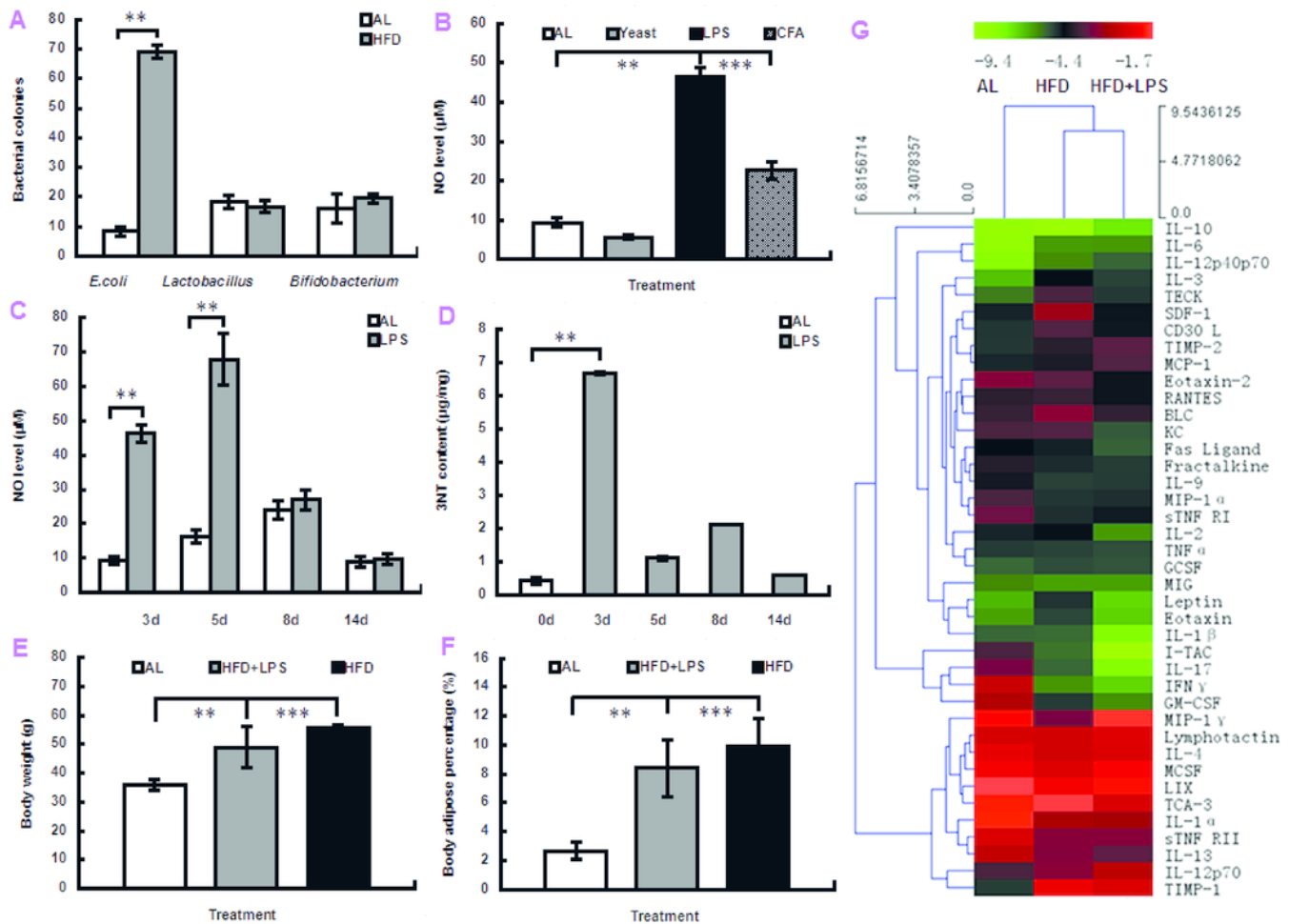
- 477 **Hawley SA, Fullerton MD, Ross FA, Schertzer JD, Chevtzoff C, Walker KJ, Peggie MW, Zibrova D,**
478 **Green KA, Mustard KJ, et al. 2012.** The ancient drug salicylate directly activates AMP-activated protein
479 kinase. *Science* **336**: 918-922
- 480 **Heinrichsdorff J, Olefsky JM. 2012.** Fetuin-A: the missing link in lipid-induced inflammation. *Nat*
481 *Med* **18**:1182-1183
- 482 **Hiernaux JR, Baker PJ, Delisi C, Rudbach JA. 1982.** Modulation of the immune response to
483 lipopolysaccharide. *J Immunol* **128**:1054-1058
- 484 **Ibrahim MI, Farghaly E, Gomaa W, Kelleni M, Abdelrahman AM. 2011.** Nitro-aspirin is a potential
485 therapy for non alcoholic fatty liver disease. *Eur J Pharmacol* **659**:289-295
- 486 **Imajo K, Fujita K, Yoneda M, Nozaki Y, Ogawa Y, Shinohara Y, Kato S, Mawatari H, Shibata W,**
487 **Kitani H, et al. 2012.** Hyperresponsivity to low-dose endotoxin during progression to nonalcoholic
488 steatohepatitis is regulated by leptin-mediated signaling. *Cell Metab* **16**:44-54
- 489 **Islam Z, Pestka JJ. 2006.** LPS priming potentiates and prolongs proinflammatory cytokine response to the
490 trichothecene deoxynivalenol in the mouse. *Toxicol Appl Pharmacol* **211**:53-63
- 491 **Jais A, Einwallner E, Sharif O, Gossens K, Lu TT, Soyak SM, Medgyesi D, Neureiter D, Paier-Pourani J,**
492 **Dalgaard K, et al. 2014.** Heme oxygenase-1 drives metaflammation and insulin resistance in mouse and
493 man. *Cell* **158**:25-40
- 494 **Kapeller R, Toker A, Cantley LC, Carpenter CL. 1995.** Phosphoinositide 3-kinase binds constitutively to
495 alpha/beta-tubulin and binds to gamma-tubulin in response to insulin. *J Biol Chem* **270**:25985-25991
- 496 **Katz DL. 2014.** Obesity is not a disease. *Nature* **508**:S57
- 497 **Kelly D, Delday MI, Mulder I. 2012.** Microbes and microbial effector molecules in treatment of
498 inflammatory disorders. *Immunol Rev* **245**:27-44
- 499 **Kim KA, Gu W, Lee IA, Joh EH, Kim DH. 2012.** High fat diet-induced gut microbiota exacerbates
500 inflammation and obesity in mice via the TLR4 signaling pathway. *PLoS One* **7**:e47713
- 501 **Pal D, Dasgupta S, Kundu R, Maitra S, Das G, Mukhopadhyay S, Ray S, Majumdar SS, Bhattacharya S.**
502 **2012.** Fetuin-A acts as an endogenous ligand of TLR4 to promote lipid-induced insulin resistance. *Nat Med*
503 **18**:1279-1285
- 504 **Pelletier A, Coderre L. 2007.** Ketone bodies alter dinitrophenol-induced glucose uptake
505 through AMPK inhibition and oxidative stress generation in adult cardiomyocytes. *Am J Physiol Endocrinol*
506 *Metab* **292**:E1325-1332

- 507 **Perry RJ, Kim T, Zhang XM, Lee HY, Pesta D, Popov VB, Zhang D, Rahimi Y, Jurczak MJ, Cline**
508 **GW, et al. 2013.** Reversal of hypertriglyceridemia, fatty liver disease, and insulin resistance by a liver-
509 targeted mitochondrial uncoupler. *Cell Metab* **18**:740-748
- 510 **Perry RJ, Zhang DY, Zhang XM, Boyer JL, Shulman GI. 2015.** Controlled-release mitochondrial
511 protonophore reverses diabetes and steatohepatitis in rats. *Science* **347**: 1253-1256.
- 512 **Petersen AM, Pedersen BK. 2005.** The anti-inflammatory effect of exercise. *J Appl Physiol* **98**: 1154–1162
- 513 **Tsuchiya K, Sakai H, Suzuki N, Iwashima F, Yoshimoto T, Shichiri M, Hirata Y.2007.** Chronic blockade
514 of nitric oxide synthesis reduces adiposity and improves insulin resistance in high fat-induced obese mice.
515 *Endocrinology* **148**:4548–4556
- 516 **Wang DT, He J, Wu M, Li SM, Gao Q, Zeng QP. 2015.** Artemisinin mimics calorie restriction to trigger
517 mitochondrial biogenesis and compromise telomere shortening in mice. *PeerJ* **3**:e822
- 518 **Wells MT, Gaffin SL, Wessels BC, Brock-Utne JG, Jordaan JP, van den Ende J. 1990.** Anti-
519 LPS antibodies reduce endotoxemia in whole body ⁶⁰Co irradiated primates: a preliminary report. *Aviat*
520 *Space Environ Med* **61**:802-806
- 521 **Yuan M, Konstantopoulos N, Lee J, Hansen L, Li ZW, Karin M, Shoelson SE. 2001.** Reversal of obesity-
522 and diet-induced insulin resistance with salicylates or targeted disruption of Ikk beta. *Science* **293**:1673-
523 1677
- 524 **Zhao L, Zhong S, Qu H, Xie Y, Cao Z, Li Q, Yang P, Varghese Z, Moorhead JF, Chen Y, Ruan XZ.**
525 **2015.** Chronic inflammation aggravates metabolic disorders of hepatic fatty acids in high-fat diet-induced
526 obese mice. *Sci Rep* **5**:10222

1

Image of obese modeling

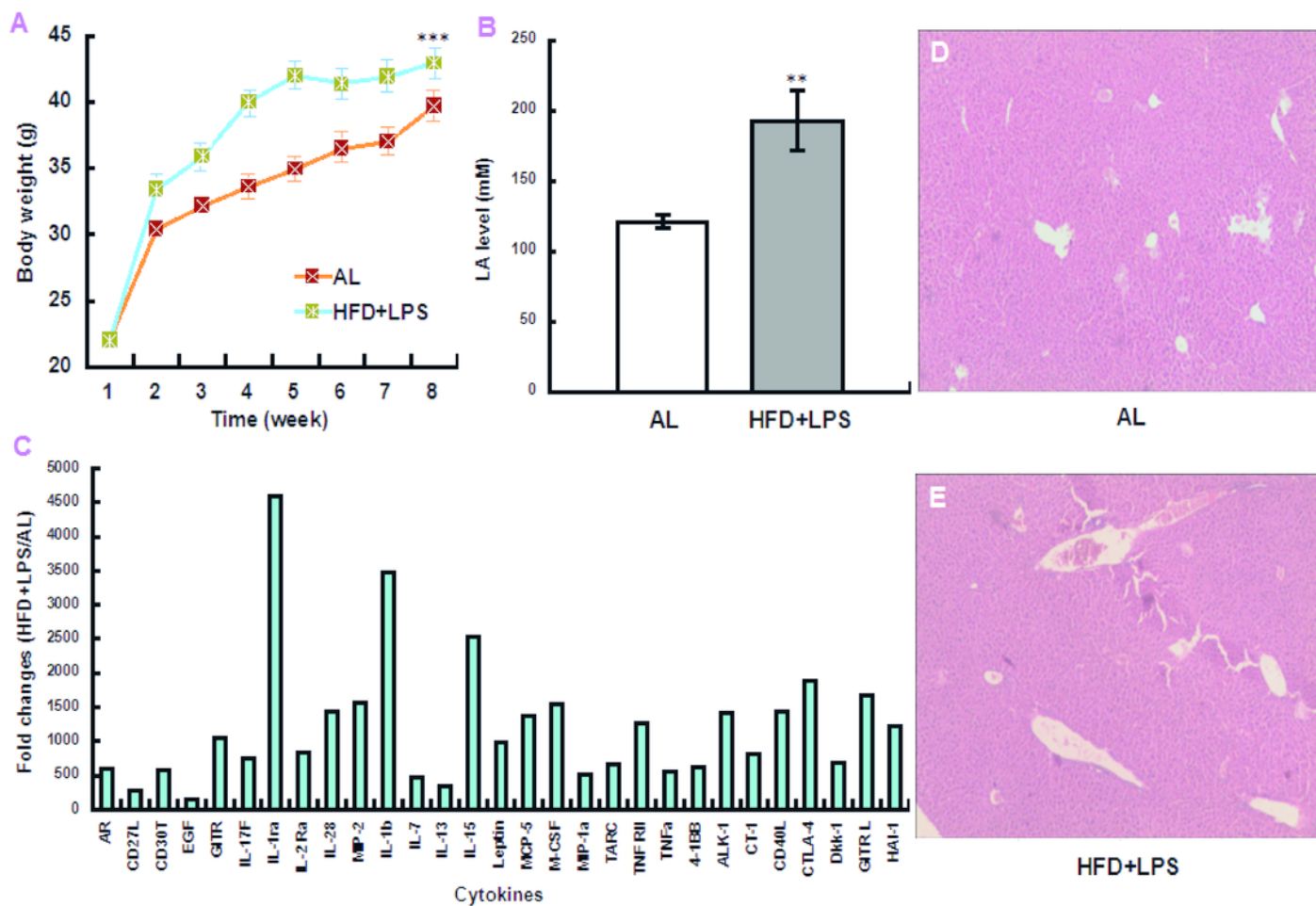
Figure 1 The modeling of obese mice without muscular inflammation by HFD or HFD+1.2 mg/kg LPS. (A) Colony counts from fecal dilutions of AL ($n=3$) and HFD mice ($n=3$) containing *E. coli*, *Lactobacillus*, and *Bifidobacterium* strains on the plates of selective EMB, LBS, and TPY media after cultured for 24 h, 72 h, and 72 h, respectively. For HFD modeling, mice were first fed with AL for two weeks and then fed with HFD for 1.5 months. (B) The serum NO level in mice fed with overnight cultured live yeast ($n=3$), or injected with 1.2 mg/kg LPS ($n=3$) or 5 mg/kg CFA ($n=3$) into hind-leg muscles. The determination was conducted on the next day after feeding or injection. (C) and (D) The serum NO level and the muscular 3NT content in AL mice and LPS-injected mice. 1.2 mg/kg LPS was injected into hind-leg muscles on the 1st, 3rd, 6th, and 12th days. The serum NO level and muscular 3NT content were determined on the 3rd, 5th, 8th, and 14th days. (E) The body weight of AL mice ($n=3$), HFD mice ($n=4$) and HFD+1.2 mg/kg LPS mice ($n=5$); (F) The body adipose percentage of AL mice ($n=4$), HFD mice ($n=5$) and HFD+1.2 mg/kg LPS mice ($n=6$). (G) A schematic diagram of hierarchical clustering for the up/down-regulation of 40 cytokines/chemokines in the muscular tissue of AL mice ($n=1$), HFD mice ($n=1$) and HFD+1.2 mg/kg LPS mice ($n=1$) by the cytokine antibody array. The red color represents upregulation as compared with AL, and the green color represents downregulation as compared with AL. HFD mice were first fed with AL for two weeks and then fed with HFD for two months. HFD+1.2 mg/kg LPS mice were first fed with AL for two weeks and then fed with HFD for two months, during which 1.2 mg/kg LPS was injected into hind-leg muscles one day before sampling.



2

Image of inflammatory modeling

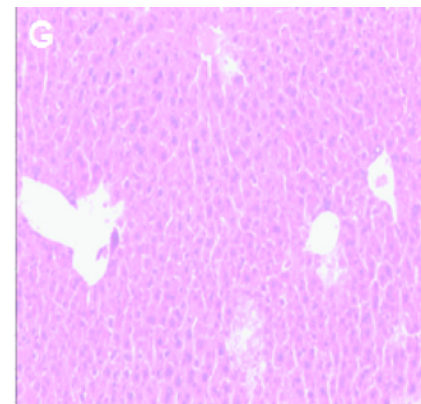
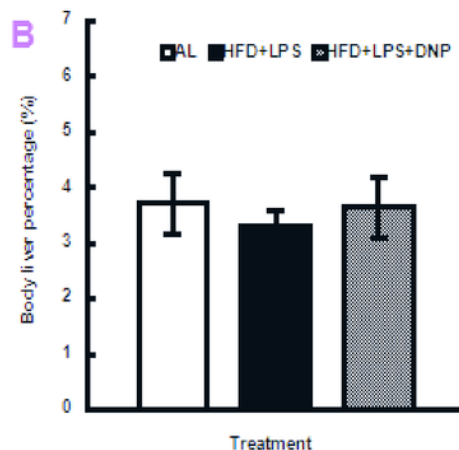
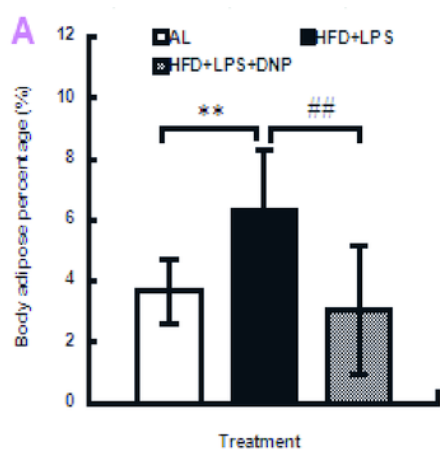
Figure 2 The modeling of obese mice with hepatic low-grade inflammation by HFD+low-dose LPS. (A) A body weight curve of AL mice ($n=16$) and HFD+0.25 mg/kg LPS mice ($n=14$). (B) The LA levels in the serum of AL mice ($n=3$) and HFD+0.25 mg/kg LPS mice ($n=3$). (C) The fold changes of cytokines/chemokines with above 100-fold upregulation in the adipose tissue of HFD+0.25 mg/kg LPS mice ($n=1$) compared with AL mice ($n=1$). (D) and (E) The histochemical staining of hepatic inflammatory pathogenesis (4×10) in AL mice and HFD+0.25 mg/kg LPS mice. HFD+0.25 mg/kg LPS mice were first fed with AL for two weeks and then fed with HFD for 1.5 months, during which 0.25 mg/kg LPS was injected into peritoneal from the 5th week on every two days for two weeks. All measurements and analysis were carried out after the completion of modeling for eight weeks.



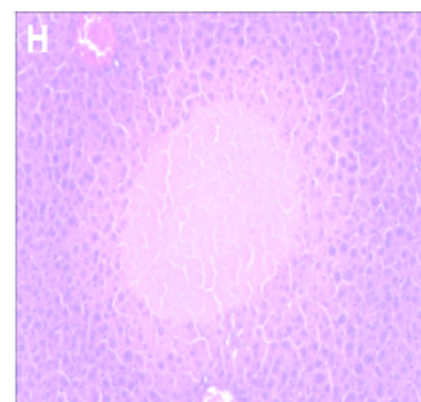
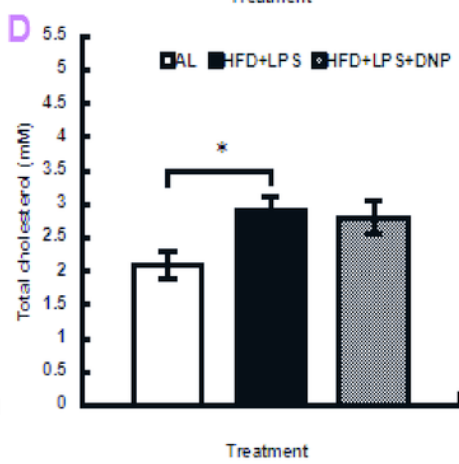
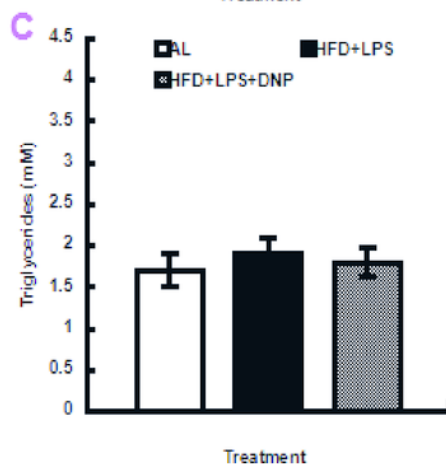
3

Image of identification

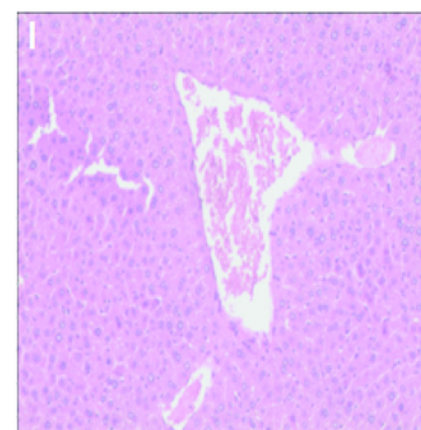
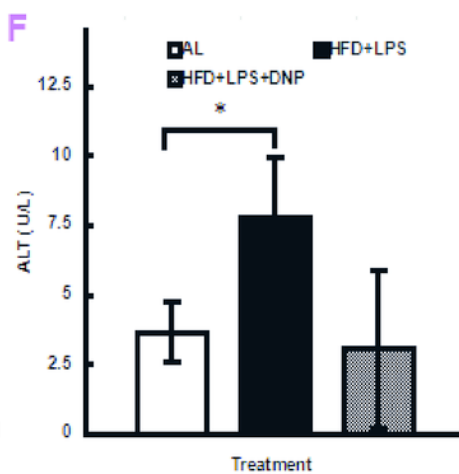
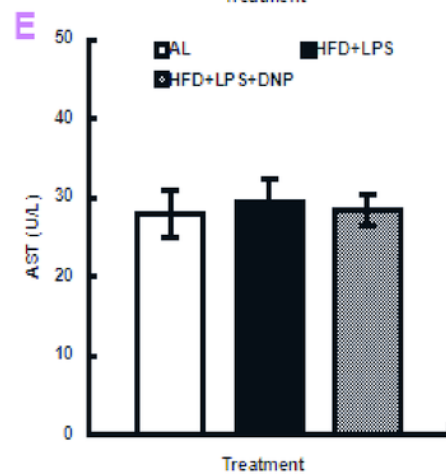
Figure 3 The phenotypic, serological, and histochemical identification in HFD+0.25 mg/kg LPS-induced obese mice after treatment by 1.6 mg/kg DNP. (A) and (B) The body adipose and body liver percentages; (C) and (D) The serum triglycerides and total cholesterol concentrations; (E) and (F) The serum AST and ALT titers; (G)-(I) HE staining of the hepatic tissue (10×10) in AL, HFD+0.25 mg/kg LPS, and HFD+0.25 mg/kg LPS+1.6 mg/kg DNP mice. HFD+0.25 mg/kg LPS mice were first fed with AL for two weeks and then fed with HFD for 1.5 months, during which 0.25 mg/kg LPS was intraperitoneally injected from the 5th week on every two days for two weeks. The obese mice were injected into peritoneal daily by 16 mg/kg DNP for two weeks.



AL



HFD+LPS

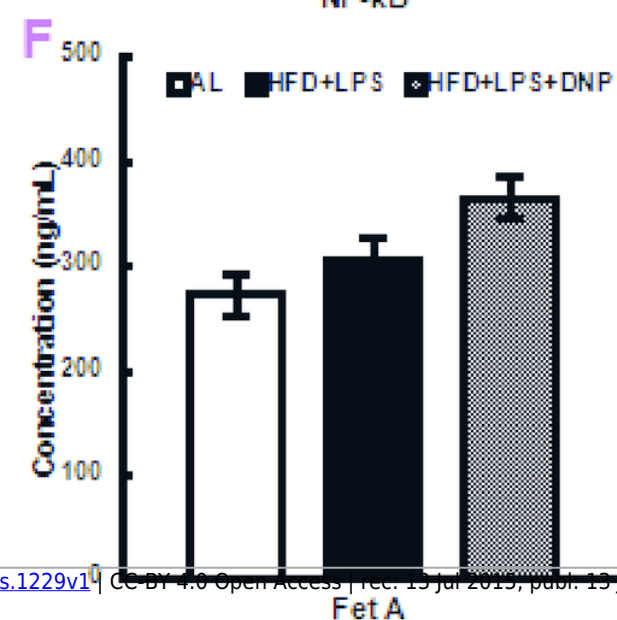
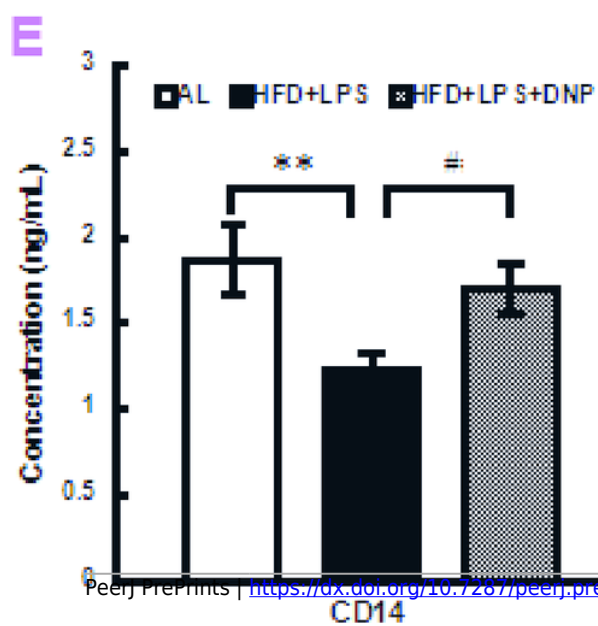
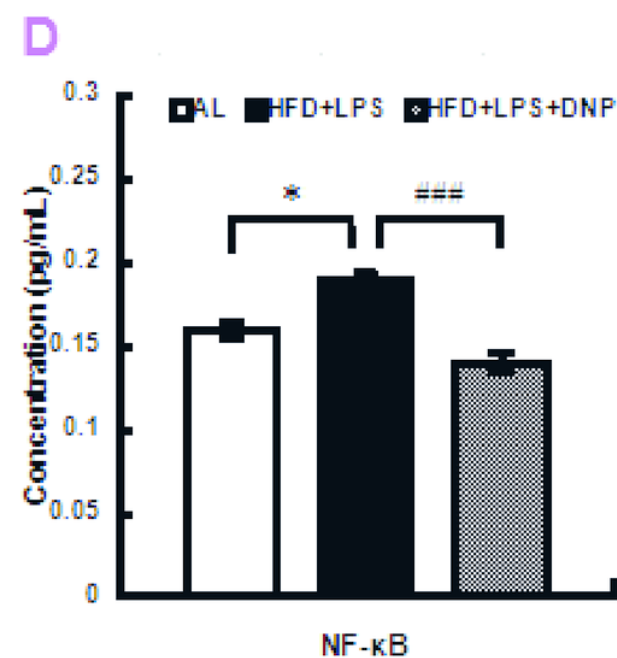
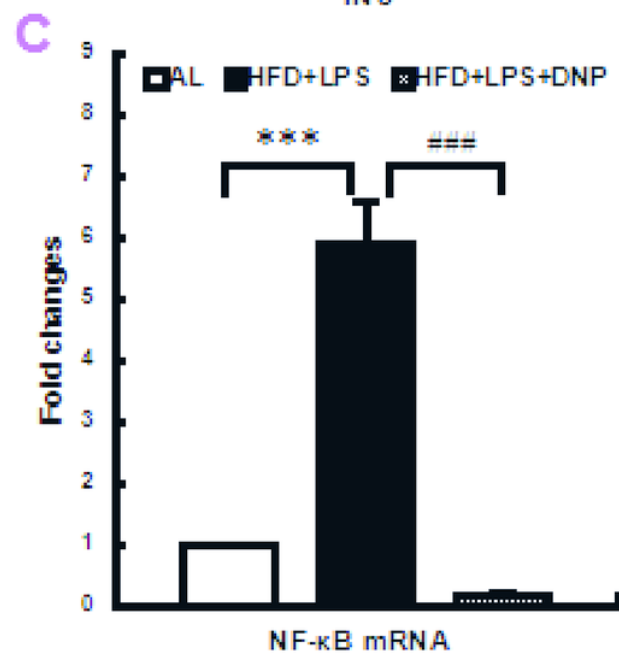
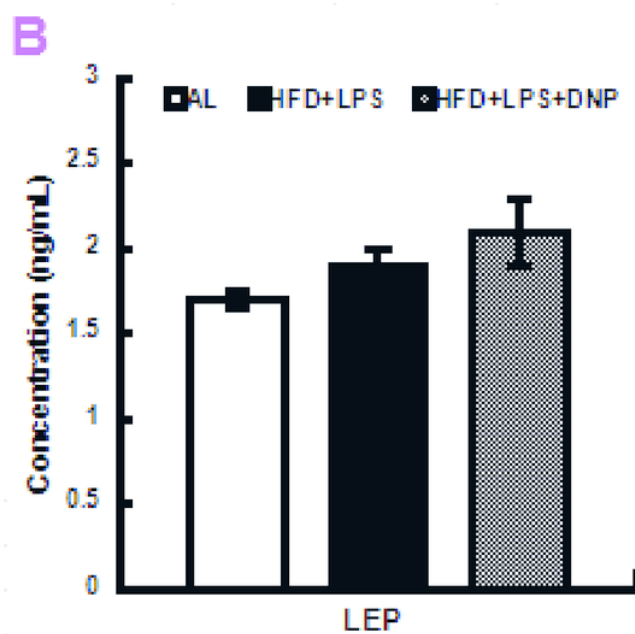
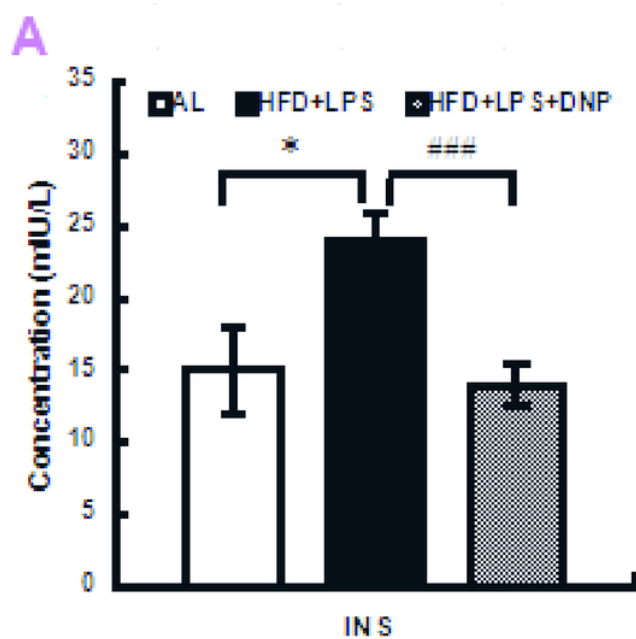


HFD+LPS+DNP

4

Image of profiling

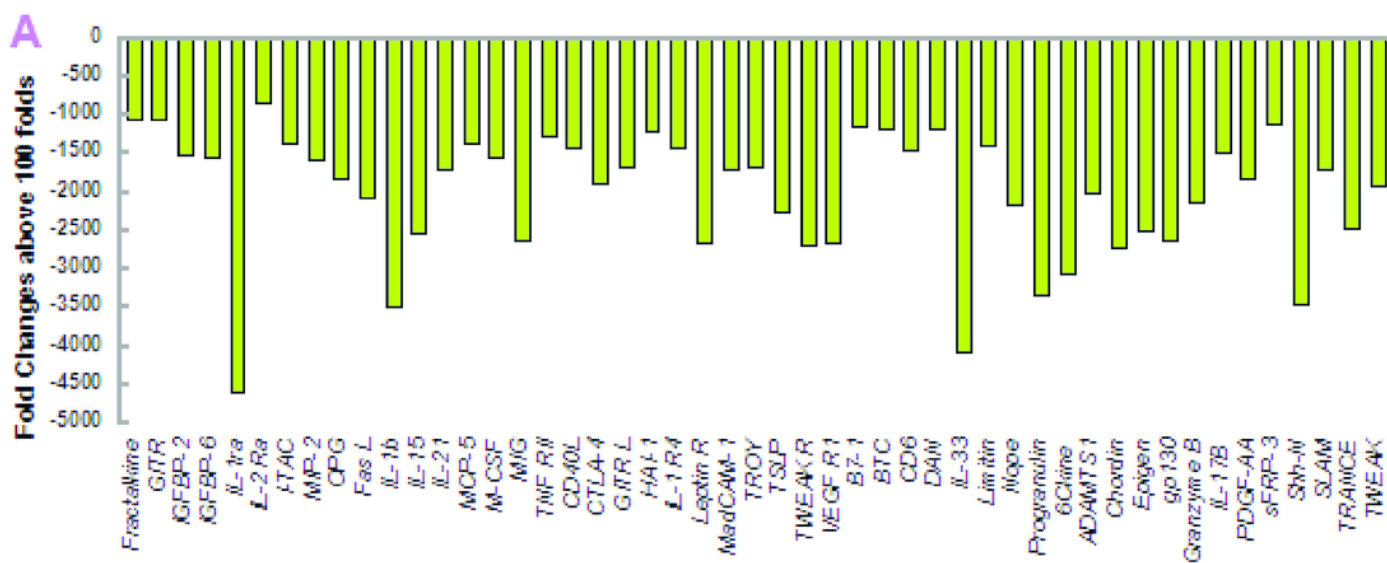
Figure 4 The expression profiling of insulin, leptin, NF- κ B, CD14, and Fet A in HFD+0.25 mg/kg LPS-induced obese mice treated by 1.6 mg/kg DNP. (A) The serum INS concentration determined by ELISA; (B) The serum LEP concentration determined by ELISA; (C) The fold changes of hepatic NF- κ B mRNA quantified by qPCR; (D) The hepatic NF- κ B concentration determined by ELISA; (E) The hepatic CD14 concentration determined by ELISA; and (G) The hepatic Fet A concentration determined by ELISA. HFD+0.25 mg/kg LPS mice were first fed with AL for two weeks and then fed with HFD for 1.5 months, during which 0.25 mg/kg LPS was intraperitoneally injected from the 5th week on every two days for two weeks. The obese mice were injected into peritoneal daily by 16 mg/kg DNP for two weeks.



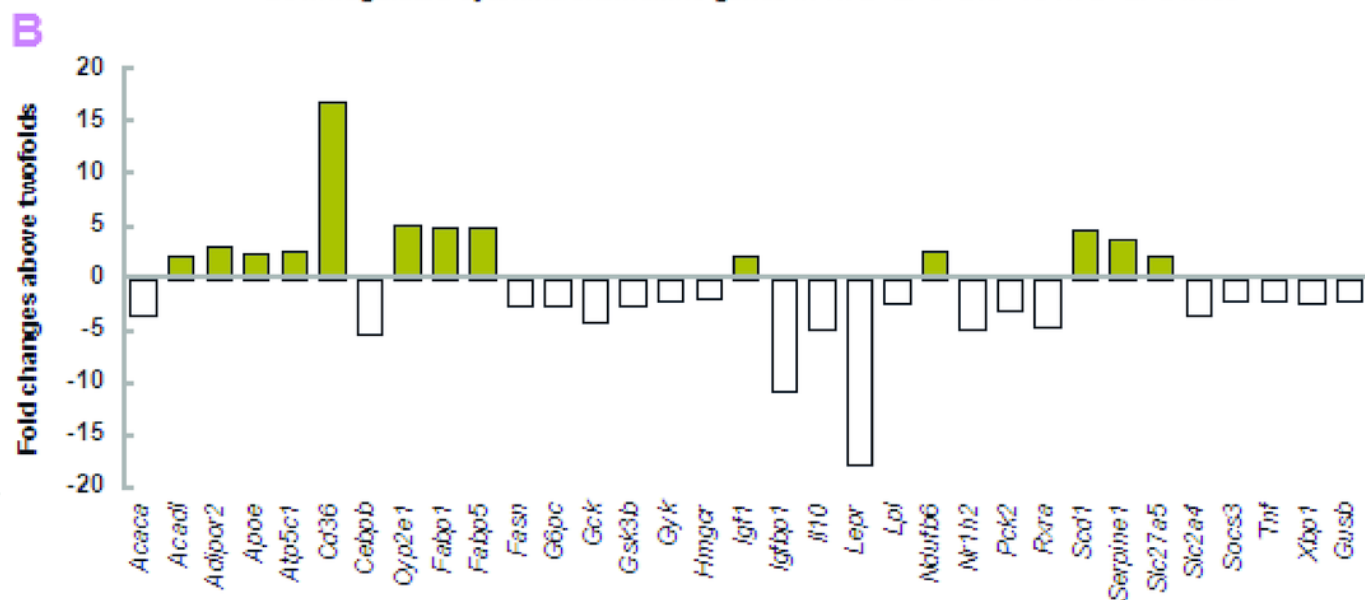
5

Image of downregulation

Figure 5 The fold changes of downregulated cytokines/chemokines and NALFD genes by 1.6 mg/kg DNP in HFD+0.25 mg/kg LPS-induced obese mice. (A) DNP-downregulated cytokines/chemokines in the adipose tissue of obese mice; (B) DNP-up/downregulated NALFD genes in the hepatic tissue of obese mice. HFD+0.25 mg/kg LPS mice were first fed with AL for two weeks and then fed with HFD for 1.5 months, during which 0.25 mg/kg LPS was intraperitoneally injected from the 5th week on every two days for two weeks. The obese mice were injected into peritoneal daily by 16 mg/kg DNP for two weeks.



Downregulated cytokine/chemokine genes in HFD+LPS+DNP vs HFD+LPS mice



Up/downregulation of NALFD genes in HFD+LPS+DNP vs HFD+LPS mice

Image of mechanism

Figure 6 A putative mechanism underlying LPS-driven inflammatory obesity and DNP-exerted weight loss effects. Gut dysbiosis-induced proinflammatory cytokines can activate iNOS for high-level NO production, which results in metabolic hypoxia, adipogenesis and adipose whitening. DNP can activate both AMPK and eNOS for low-level NO release, which leads to mitochondrial biogenesis and adipose browning. The red line with the symbol + represents activation; the black line with the symbol - represents inhibition.

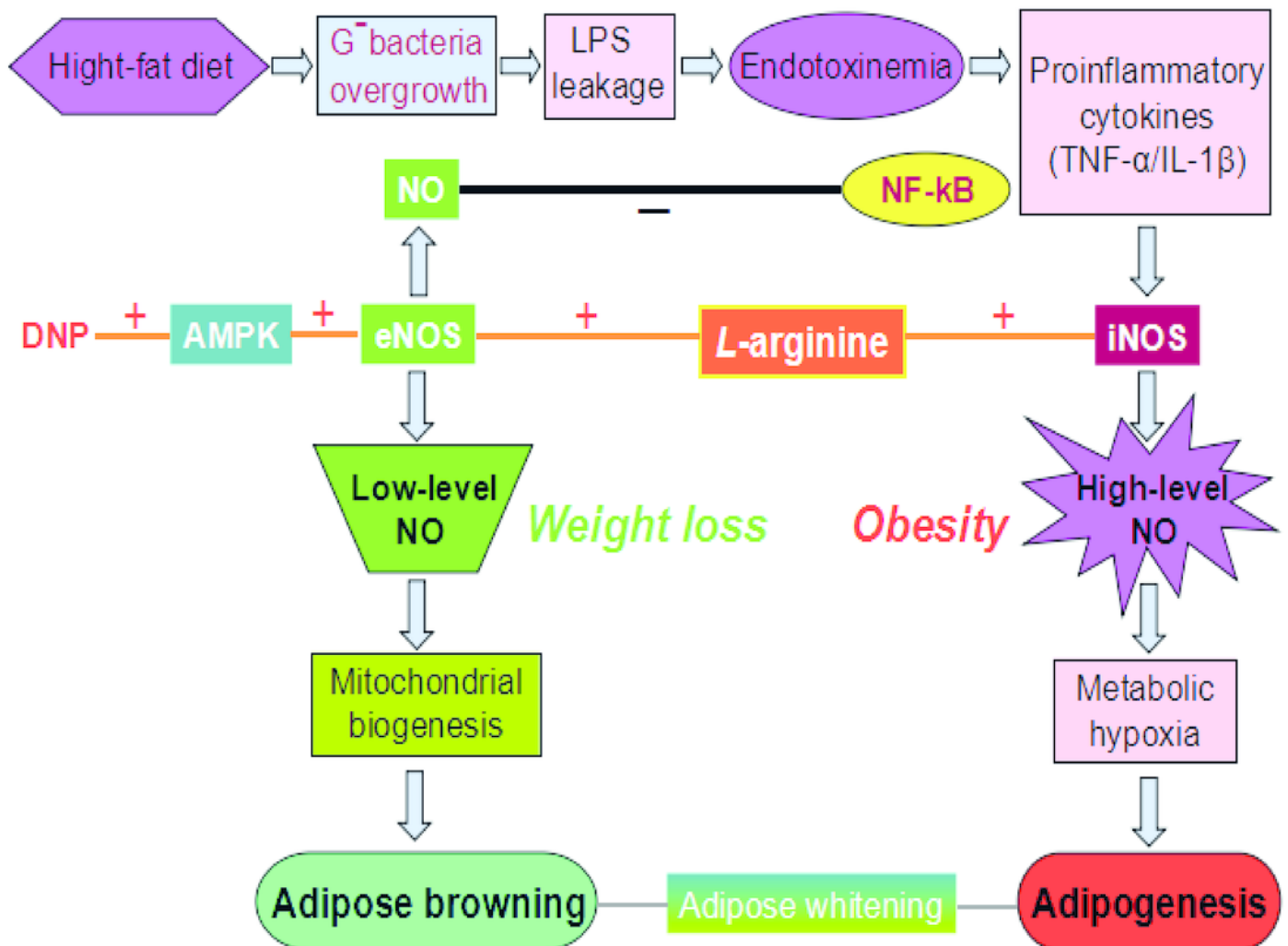


Table 1 (on next page)

List of NAFLD

Table 1 Comparison of upregulated transcripts among 84 NAFLD-related pathway genes in the hepatic tissue among AL mice, HFD mice, and HFD+1.2 mg/kg LPS mice by RT-PCR array

Notes: The fold changes were calculated from the comparison of HFD+1.2 mg/kg LPS mice versus AL mice (the 1st value), the comparison of HFD mice versus AL mice (the 2nd value), and the comparison of HFD mice versus HFD+1.2 mg/kg LPS mice (the 3rd value). The 2nd values were only listed for inflammatory response transcripts and NIDDM-involved transcripts. HFD+1.2 mg/kg LPS mice were first fed with AL for two weeks and then fed with HFD for two months, during which 1.2 mg/kg LPS was injected into hind-leg muscles one day before sampling. RT-PCR array was carried out after the completion of modeling.

Transcript category	Upregulated transcript	
	Gene	Fold change
Inflammatory response	<i>Ifng</i>	5.52/-5.21/-28.74
	<i>Il1b</i>	94.24/6.46/-14.59
	<i>Il6</i>	12.54/1.51/-8.33
	<i>Il10</i>	50.20/4.32/-11.63
	<i>Tnf</i>	10.24/1.15/-8.87
NIDDM-involved	<i>Soxs3</i>	7.18/1.56/-4.59,
	<i>Xbp1</i>	2.18/2.41/1.11
Insulin signaling pathway	<i>Igf1</i>	3.19/1.46
Adipokine signaling pathway	0	0
Metabolic pathways		
Carbohydrate metabolism	<i>G6pc</i>	3.64/72.16
	<i>Pdk4</i>	21.27/-5.53
	<i>Rbp4</i>	2.65/30.76
Fatty acid β -oxidation	<i>Acox1</i>	2.13/-1.10
	<i>Cpt1a</i>	2.72/-1.37
Cholesterol metabolism/transport	<i>Abca1</i>	6.48/-1.46
	<i>Abcg1</i>	27.10/-5.17

	<i>Apoa1</i>	2.83/320.07
	<i>Apob</i>	6.97/709.63
	<i>Cyp2e1</i>	34.38/24.94
	<i>Nr1h3</i>	3.39/-1.53
Other lipid metabolism/transport	<i>Acs15</i>	2.96/-1.36
	<i>Acsm3</i>	5.57/12.03
	<i>Fabp3</i>	2.18/-1.08
	<i>Slc27a5</i>	2.57/130.38
Oxidative phosphorylation	0	0
Apoptosis	<i>Casp3</i>	3.27/-1.27

Table 2 (on next page)

List of NIDDM

Table 2 Fold changes of hepatic inflammatory response and NIDDM transcripts in HFD+low-dose LPS mice compared with AL mice

Notes: HFD+0.25 mg/kg LPS mice were first fed with AL for two weeks and then fed with HFD for 1.5 months, during which 0.25 mg/kg LPS was injected into peritoneal from the 5th week on every two days for two weeks.

Transcript category	Gene	Fold change	
		Upregulated	Unchanged
		(above 2 folds)	(-2 folds to 2 folds)
Inflammatory response	<i>Cebpb</i>		1.75
	<i>Fas</i>	2.00	
	<i>Ifng</i>		-1.78
	<i>Il10</i>		-1.70
	<i>Il1b</i>	2.64	
	<i>Il6</i>	2.80	
	<i>Rxra</i>	2.45	
	<i>Tnf</i>		-1.39
NIDDM	<i>Gck</i>	4.38	
	<i>Insr</i>	2.01	
	<i>Irs1</i>		1.70
	<i>Mapk1(Erk2)</i>		1.02
	<i>Mapk8(Jnk1)</i>		1.14
	<i>Mtor</i>	2.71	
	<i>Pik3r1(Pi3k,P85a)</i>		-1.12
	<i>Slc2a2</i>	2.44	
	<i>Slc2a4(Glut4)</i>		-1.25
	<i>Socs3</i>	3.76	
	<i>Xbp1</i>	3.10	

1

2

Table 3(on next page)

List of DNP effects

Table 3 Comparison of DNP effects on the expression of NIDDM transcripts among HFD+0.25mg/kg LPS+16 mg/kg DNP mice, HFD+0.25 mg/kg LPS mice, and AL mice

Notes: HFD+0.25 mg/kg LPS mice were first fed with AL for two weeks and then fed with HFD for 1.5 months, during which 0.25 mg/kg LPS was intraperitoneally injected from the 5th week on every two days for two weeks. The obese mice were intraperitoneally injected daily by 16 mg/kg DNP for two weeks.

NIDDM transcript	HFD+LPS+DNP vs HFD+LPS	HFD+LPS+DNP vs AL
<i>Gck</i>	-4.29	1.02
<i>Insr</i>	-1.52	1.36
<i>Irs1</i>	-1.25	1.31
<i>Mapk1 (Erk2)</i>	-1.01	1.00
<i>Mapk8(Jnk1)</i>	-1.47	-1.32
<i>Mtor</i>	-1.19	2.27
<i>Pik3ca (p110A)</i>	1.04	1.23
<i>Pik3r1 (Pi3k p85α)</i>	3.4	3.08
<i>Pklr</i>	-1.58	-1.06
<i>Slc2a4 (Glut4)</i>	-3.62	-4.52
<i>Slc2a2</i>	-1.81	1.33
<i>Socs3</i>	-2.06	1.87
<i>Tnf</i>	-2.17	-3.08
<i>Xbp1</i>	-2.38	1.30
